J Arid Land (2025) 17(11): 1518–1541
doi: 10.1007/s40333-025-0111-x; CSTR: 32276.14.JAL.0250111x

Science Press Springer-Verlag

Enhancing ecological network connectivity in semi-arid mountain areas through minimal landscape restructuring

PAN Yilu[1,2], YANG Xia[1,2], FANG Yuxuan[1,2], PAN Hongyi[1,2*], ZHANG Wen[3]

[1] Faculty of Geography and Resources Sciences, Sichuan Normal University, Chengdu 610066, China;
[2] Key Laboratory of Land Resources Evaluation and Monitoring in Southwest, Ministry of Education, Chengdu 610066, China;
[3] School of Civil Engineering and Water Resources, Qinghai University, Xining 810016, China

Abstract: Increasing human disturbance and climate change have threatened ecological connectivity and structural stability, especially in semi-arid mountain areas with sparse vegetation and weak hydrological regulation. Large-scale ecological restoration, such as adding ecological sources or corridors, is difficult in such environments and often faces poor operability and high implementation costs in practice. Taking the southern slope of the Qilian Mountains in China as the study area and 2020 as the baseline, this study integrated weighted complex network theory into the "ecological source–resistance surface–corridor" framework to construct a heterogeneous ecological network (EN). Circuit theory was integrated with weighted betweenness to identify critical barrier points for locally differentiated restoration, followed by assessment of the network optimization effects. The results revealed that 494 ecological sources and 1308 ecological corridors were identified in the study area. Fifty-one barrier points with restoration potential were identified along key ecological corridors and locally restored. After optimization, the network gained 11 additional ecological corridors, and the total ecological corridor length increased by approximately 1143 km. Under simulated attacks, the decline rates of maximum connected subgraph (MCS) and network efficiency (Ne) slowed compared with pre-restoration conditions, indicating improved robustness. These findings demonstrate that targeted local restoration can enhance network connectivity and stability while minimizing disturbance to the overall landscape pattern, providing a practical pathway for ecological restoration and sustainable management in semi-arid mountain areas.

Keywords: ecological networks; circuit theory; complex networks; gravity model; ecosystem services; ecological source; ecological barrier point

Citation: PAN Yilu, YANG Xia, FANG Yuxuan, PAN Hongyi, ZHANG Wen. 2025. Enhancing ecological network connectivity in semi-arid mountain areas through minimal landscape restructuring. Journal of Arid Land, 17(11): 1518–1541. https://doi.org/10.1007/s40333-025-0111-x; https://cstr.cn/32276.14.JAL.0250111x

1 Introduction

Recent rapid urbanization and intensified human activities have led to significant ecological degradation (Shen et al., 2024; Huang et al., 2025). Arid and semi-arid areas are highly sensitive to intensifying environmental pressures, hosting fragile ecosystems whose conditions are critical to regional stability and sustainable development (Sui et al., 2024). Ecological vulnerability further heightens the risks of habitat fragmentation and declining connectivity, threatening ecosystem

*Corresponding author: PAN Hongyi (E-mail: panhongyi80@sicnu.edu.cn)
Received 2025-06-05; revised 2025-09-24; accepted 2025-10-31

integrity and biodiversity (Gu et al., 2024; Zhang et al., 2024b). As a key spatial framework that links fragmented habitats and sustains ecological functions, ecological networks (ENs) have thus become a major focus for maintaining and enhancing landscape connectivity (Shen et al., 2022; Liang et al., 2023; Chen et al., 2025a).

ENs are an integrated outcome of island biogeography theory, metapopulation theory, and landscape ecology (Gao et al., 2024b). They represent a comprehensive approach to systematically maintaining ecological balance and promoting sustainability. Currently, extensive studies have led to the widespread adoption of a standardized framework for EN construction "source identification–resistance surface construction–corridor extraction" (Huang et al., 2021; Yang et al., 2022b; Jiang et al., 2024b). Ecological sources, which support ecological functions such as ecosystem service provision, species dispersal, and genetic exchange (Nie et al., 2024), are often characterized by rich natural resources and high biodiversity. Ecological sources can be identified either by selecting large and contiguous ecological lands such as nature reserves (Sun et al., 2024a), or through composite methods that integrate Morphological Spatial Pattern Analysis (MSPA) (Ye et al., 2020), ecosystem service importance (Liu et al., 2024), landscape connectivity (Wei et al., 2022; Yin et al., 2025), and ecological sensitivity (Liu et al., 2023b). The resistance surface, typically constructed based on land cover, topography, and anthropogenic disturbance, quantifies the difficulty of species movement across landscapes (Guo et al., 2025). Ecological corridors, linear or belt-shaped elements connecting ecological sources (West et al., 2016), are commonly extracted using approaches such as Minimum Cumulative Resistance (MCR) model (Fu et al., 2024; Qi et al., 2025), circuit theory (Zhang et al., 2024a; Qu et al., 2025), or ant colony optimization algorithms (Pan et al., 2023). In addition, the gravity model is frequently applied to evaluate corridor importance (Luo et al., 2024; Chen et al., 2025b). This framework has been extensively applied across different spatial scales to support EN design and analysis.

Complex network theory, derived from graph theory and developed through studies of real-world systems such as social, technological, and biological networks (Albert and Barabási, 2002), provides a powerful framework for EN research. By abstracting ecological sources as nodes and corridors as edges (Yu et al., 2018), the complex network framework enables a systematic assessment of network topology, including connectivity, robustness, and vulnerability (Tong et al., 2025). Compared with MCR or circuit theory, complex network analysis integrates structural and functional attributes to reveal critical nodes and corridors often missed by other approaches (Fenu and Pau, 2018; Gao et al., 2024c), thereby informing optimization strategies (Liu et al., 2023a). However, most applications still rely on unweighted networks that ignore differences in connection strength and ecological importance (Barrat et al., 2004). Although recent studies have introduced weights to reflect ecosystem heterogeneity (Gao et al., 2023), topological analysis often reverts to unweighted forms and underestimates key corridors (Costa et al., 2019). Weighted edge betweenness overcomes this limitation by incorporating edge weights into shortest-path calculations (Estrada and Bodin, 2008), capturing both connection strength and structural position and providing a more accurate basis for EN optimization.

In recent years, EN studies have increasingly focused on maintaining or enhancing specific ecological functions within defined regions. For example, Jiang et al. (2022) highlighted a zoned ecological restoration strategy that specifies protection targets and restoration priorities for different areas to achieve coordinated conservation and differentiated management. Zhao et al. (2023) integrated local ecosystem functions with connectivity objectives to develop targeted optimization strategies for disturbed mining areas. Hong et al. (2025) introduced a local-world network model that incorporates geographic constraints when adding new ecological sources and corridors, addressing the needs of densely developed urban areas. In arid and semi-arid areas, however, large-scale structural reconstruction is often constrained by intensive land use (Cao et al., 2024), spatial limitations (Jiang et al., 2024a), and high implementation costs (Beltrão et al., 2024). Moreover, barrier zones within existing networks are rarely restored; added corridors or sources typically bypass or replace obstructed routes, leaving original paths functionally impaired and ecologically isolated. To address these issues, we proposed and emphasized a more direct local restoration pathway: integrating weighted complex network analysis with circuit theory to identify

high-resistance segments along key corridors and prioritizing ecological restoration in barrier zones that meet restoration criteria, thereby restoring the accessibility and functionality of the original ecological pathways. Compared with merely adding alternative corridors, local restoration more effectively removes resistance sources and enhances the functionality of existing corridors while minimizing disturbance to the overall landscape pattern and strengthening network robustness and stability.

Located in the semi-arid–arid transition of Northwest China, the southern slope of the Qilian Mountains forms a vital ecological barrier supporting regional water conservation and ecological security. The area's fragile environmental foundation has faced mounting ecological stress in recent decades, including reduced water-conservation capacity (Wei et al., 2023), glacier retreat (He et al., 2019), and grassland degradation (Qian et al., 2021), all of which threaten long-term landscape stability. These inherent constraints make large-scale ecological restoration projects difficult to implement effectively, underscoring the need for locally differentiated strategies to enhance EN connectivity while maintaining existing landscape patterns. Accordingly, this study aims to: (1) construct an EN for the southern slope of the Qilian Mountains using the "ecological source–resistance surface–corridor" framework; (2) enhance the connectivity of key corridors through localized resistance adjustment without significantly altering landscape configuration; and (3) quantify the structural and functional improvements of the optimized network using complex network metrics, thereby providing scientific guidance for ecological restoration and sustainable management in semi-arid mountain areas.

2 Study area and data sources

2.1 Study area

The southern slope of the Qilian Mountains (36°44′–39°12′N, 96°56′–102°38′E) is located at the junction of the Qinghai-Xizang Plateau, the Loess Plateau, and the Mongolian Plateau, encompassing Menyuan Hui Autonomous County, Qilian County, Gangcha County, Haiyan County, and Tianjun County in Qinghai Province, China (Xiang et al., 2024). Covering approximately 60,010 km^2 with a mean elevation of about 3800 m, the terrain is high in the northwest and lower toward the southeast (Fig. 1). The region experiences a typical plateau continental climate characterized by long and cold winters, short and cool summers, and strong solar radiation (Fu et al., 2020). Vegetation is dominated by alpine meadows, alpine steppes, alpine shrubs, and coniferous forests (Zhao et al., 2005; Zhang et al., 2025). As a core part of the Qilian Mountains National Nature Reserve, this region supports rich biodiversity and provides critical habitats for species such as snow leopards (*Panthera uncia*) and Tibetan antelopes (*Pantholops hodgsonii*). The total population is about 2.85×10^5, with local livelihoods mainly dependent on animal husbandry and eco-tourism, and the principal crops are highland barley, potatoes, and rapeseed cultivated primarily in river valleys and low-elevation basins. In recent years, ecological problems such as grassland degradation and glacier retreat have become increasingly prominent, highlighting the urgency of effective ecological management.

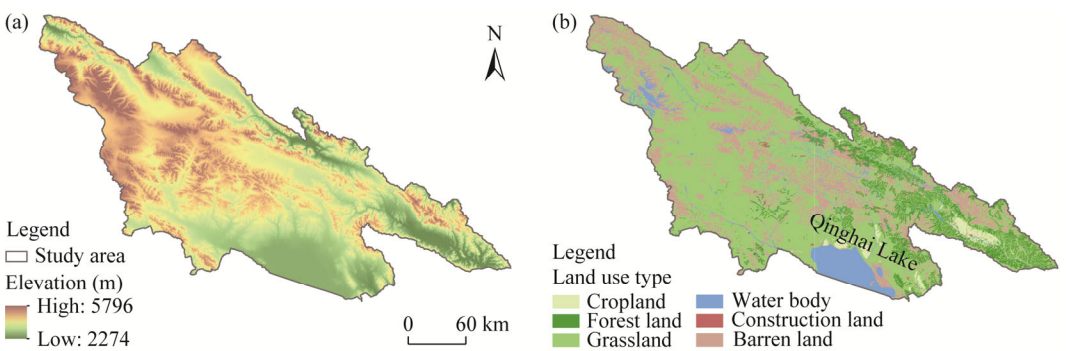

Fig. 1 Elevation (a) and land use type (b) of the southern slope of the Qilian Mountains

2.2 Data sources and processing

The datasets used in this study are summarized in Table 1, all referenced to the year 2020. Land use data were processed using a secondary classification system. To ensure data consistency and analytical precision, we reprojected all datasets to the World Geodetic System 1984, Universal Transverse Mercator Zone 48N coordinate system. Raster data were resampled to a spatial resolution of 30 m to meet the requirements of subsequent analyses.

Table 1 Detailed description of data used in this study

Data	Type	Resolution	Source
Land cover	Raster	30 m	Resource and Environmental Science and Data Platform (https://www.resdc.cn)
Digital elevation model (DEM)	Raster	30 m	Geospatial Data Cloud (https://www.gscloud.cn)
Slope	Raster	90 m	Geospatial Data Cloud (https://www.gscloud.cn)
Normalized difference vegetation index (NDVI)	Raster	30 m	National Aeronautics and Space Administration (NASA) Earth Observation Data (https://www.earthdata.nasa.gov)
Net primary productivity (NPP)	Raster	1 km	NASA Earth Observation Data (https://www.earthdata.nasa.gov)
Precipitation	Raster	1 km	National Earth System Science Data Center (http://www.geodata.cn)
Road network	Vector	-	OpenStreetMap (https://www.openstreetmap.org)
Administrative boundary	Vector	-	Resource and Environmental Science and Data Platform (https://www.resdc.cn)

Note: "-" means no resolution.

3 Methodology

To intuitively illustrate the overall concept and technical approach of this study, we developed a research framework diagram to clarify the logical relationships and operational processes among the various components (Fig. 2). The research framework comprises three main modules: (1) EN construction, integrating ecosystem service assessment and MSPA to identify ecological sources, and extracting ecological corridors using MCR model based on a composite resistance surface; (2) EN optimization, applying circuit theory and weighted complex network analysis to locate barrier points and prioritize corridor restoration through localized resistance adjustment; and (3) EN evaluation, assessing the enhanced network's robustness using the weight of the maximum connected subgraph and network efficiency.

3.1 EN construction

3.1.1 Identification of ecological sources

Ecological sources, characterized by high stability and low vulnerability, serve as critical hubs for species dispersal, energy flow, and material exchange, thereby supporting key ecological processes (Wang et al., 2025a). To determine the key ecological sources within the ENs, we combined the core areas extracted by MSPA with the regions of high ecosystem service importance identified through ecosystem service evaluation in an equal-weight manner.

MSPA is a method based on mathematical morphology for identifying and classifying landscape element types and spatial structures (Xu et al., 2023). In this study, we applied MSPA to binarize land cover data to extract core landscape components, defining forest land, high-cover grassland, water bodies, and wetlands as foreground elements, with all other land cover types treated as background (Guan et al., 2024). To extract the core areas, we set the edge width to 30 m.

We adjusted the unit value equivalent factors for provisioning (food production, material production, and water supply), regulating (air quality regulation, climate regulation, waste treatment, and regulation of water flow), supporting (erosion prevention, maintenance of soil fertility, and habitat services), and cultural (cultural and amenity services) services based on local

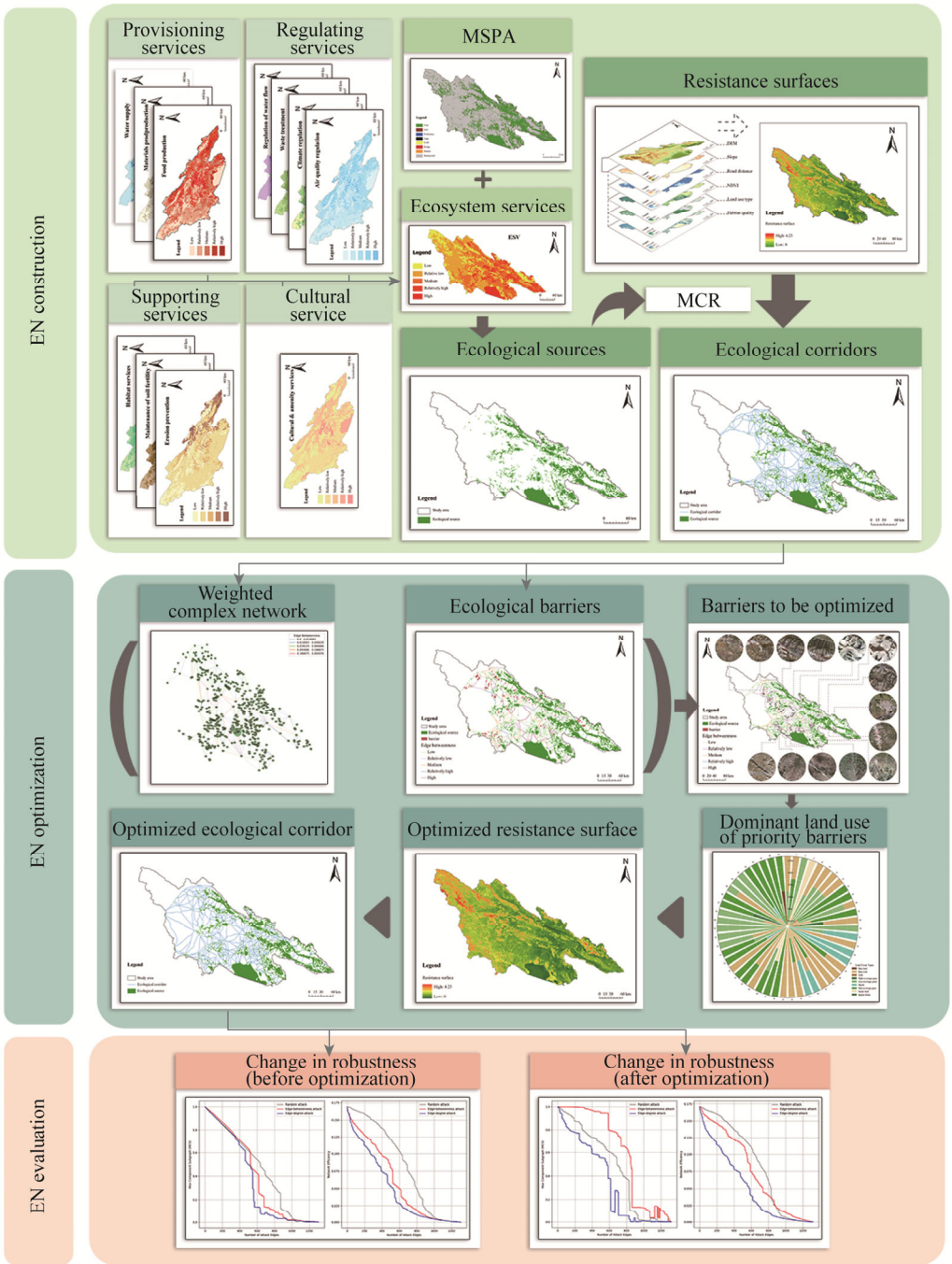

Fig. 2 Framework for construction, optimization, and evaluation of ecological networks (ENs). MSPA, morphological spatial pattern analysis; MCR, minimum cumulative resistance.

conditions, and further corrected them using net primary productivity (NPP), precipitation, and soil retention (SR) (He et al., 2023). The different services were then equally weighted and aggregated to obtain the overall ecosystem service values, thereby identifying areas with high ecosystem service importance as candidate ecological sources. SR was calculated with the Revised Universal Soil Loss Equation (RUSLE) (Gong et al., 2022; Jiang et al., 2024b). The calculation formula is as follows:

$$F_{fpq} = \begin{cases} J_{pq} \times F_{f1} = B_{pq} / \overline{B} \times F_{f1} \\ O_{pq} \times F_{f2} = W_{pq} / \overline{W} \times F_{f2} \\ T_{pq} \times F_{f3} = E_{pq} / \overline{E} \times F_{f3} \end{cases}, \quad (1)$$

where F_{fpq} is the unit area value equivalent factor of the f^{th} type of ecosystem service function in the p^{th} year of the q^{th} region of a certain ecosystem; J_{pq}, O_{pq}, and T_{pq} are the spatiotemporal adjustment factors of NPP, precipitation, and SR, respectively, in the p^{th} year of the q^{th} region of the study ecosystem; B_{pq}, W_{pq}, and E_{pq} are the per unit area NPP (t/hm^2), precipitation (mm/hm^2), and SR (t/hm^2), respectively, in the p^{th} year of the q^{th} region of a certain ecosystem; F_f is the value coefficient of the f^{th} ecosystem service in the study ecosystem, where f_1, f_2, and f_3 correspond to the ecosystem service functions related to NPP, precipitation, and SR, respectively; and $\overline{B}$, $\overline{W}$, and $\overline{E}$ represent the average NPP per unit area (t/hm^2), the mean annual precipitation per unit area (mm/hm^2), and the average simulated amount of SR per unit area (t/hm^2), respectively, for each type of ecosystem service.

$$\mathrm{SR} = (R \times K \times LS) - (R \times K \times LS \times C \times P), \quad (2)$$

where SR is the soil retention (t/(hm^2·a)); R is the rainfall erosivity factor (MJ mm/(hm^2·h·a)); K is the soil erodibility factor (t h/(MJ·mm)); LS is the topographic factor; C is the cover management factor; and P is the support practice factor.

To validate the rationality of the equivalent coefficients, we introduced the coefficient of sensitivity (CS), which characterizes the responsiveness of the total ecosystem service value to variations in value coefficients (Guo et al., 2022). The calculation formula is as follows:

$$\mathrm{CS} = \frac{\left(ES_e - ES_s\right)/ES_s \times 100\%}{\left(VC_{ek} - VC_{sk}\right)/VC_{sk} \times 100\%}, \quad (3)$$

where ES_s and ES_e are the estimated initial ecosystem service value and the adjusted ecosystem service value, respectively; and VC_{sk} and VC_{ek} are the initial ecosystem service coefficient and the adjusted ecosystem service coefficient, respectively.

3.1.2 Construction of resistance surface

The resistance surface is a simulated layer that reflects the spatial heterogeneity of resistance encountered by organisms during migration or dispersal across the landscape (Wei et al., 2025). We selected habitat quality, digital elevation model (DEM), normalized difference vegetation index (NDVI), distance to road, slope, and land use type as resistance factors for constructing the resistance surface (Lu et al., 2024; Zhang and Wang, 2024). A uniform weighting approach was applied to integrate these factors into a composite resistance surface, considering their relative importance (Yang et al., 2022a; Gao et al., 2024a; Wei et al., 2024). Habitat quality was derived using the Integrated Valuation of Ecosystem Services and Tradeoffs (InVEST) model, with the calculation expressed by the following formula (Zhao et al., 2022):

$$Q_{xy} = H_y \left[1 - \left(\frac{D_{xy}^z}{D_{xy}^z + \mathrm{k}^z}\right)\right], \quad (4)$$

where Q_{xy} is the habitat quality index of pixel x in land use type y; H_y is the habitat suitability of land use type y, with a relative suitability score ranging from 0 to 1; k is the half-saturation constant; z is the inherent conversion coefficient of the system with a value of 0.5; and D_{xy} is the level of habitat degradation for pixel x in land use type y.

3.1.3 Extraction of ecological corridors

Ecological corridors serve as vital pathways connecting ecological sources, playing a key role in facilitating material circulation and energy flow within ecosystems (Wang et al., 2022b). MCR model is commonly employed to extract ecological corridors. By calculating the least-cost paths between ecological source areas, MCR model characterizes the diffusion processes of landscape elements and evaluates the resistance effects across different landscape units, thereby assessing the

connectivity and accessibility between ecological source points (Chen et al., 2022). The calculation formula is as follows:

$$\mathrm{MCR} = f(\min)\sum_{h=m'}^{g=m}(D_{gh}\times R_g), \tag{5}$$

where f is an unknown positive function used to describe the positive correlation between the minimum resistance at any point in space and its distance to all ecological sources as well as the characteristics of the landscape matrix; D_{gh} is the spatial distance for a species to move from ecological source h to a certain point across the landscape g; R_g is the resistance of landscape g to species movement; m is the number of basic landscape units; and m' is the number of ecological source points.

The gravity model is a classical model used to characterize the interaction strength between spatial units. Originally derived from the law of universal gravitation in physics, it is commonly applied in ecology to simulate the potential mutual attraction between ecological sources (Wanghe et al., 2020). This model effectively quantifies the strength of attraction between ecological sources, assigning weights to ecological corridors and improving the authenticity of ecological process simulations. The calculation formula is as follows:

$$G_{ab} = \frac{N_a \times N_b}{D_{ab}^2} = \frac{\left(\frac{1}{P_a}\times \ln S_a\right)\left(\frac{1}{P_b}\ln S_b\right)}{\left(\frac{L_{ab}}{L_{\max}}\right)^2} = \frac{L_{\max}^2 \ln S_a \ln S_b}{L_{ab}^2 P_a P_b}, \tag{6}$$

where G_{ab} is the interaction force between ecological sources a and b, which corresponds to the weight of the ecological corridor between a and b; N_a and N_b are the weight values of ecological sources a and b, respectively; D_{ab} is the normalized cumulative resistance of the potential corridor from point a to point b; L_{ab} is the cumulative resistance value of the potential ecological corridor from point a to point b; $L_{\max}$ is the maximum cumulative resistance value within the study area; P_a and P_b are the resistance values of the ecological sources a and b, respectively; and S_a and S_b are the area of the ecological sources a and b (km^2), respectively. The value of N_a can be derived from the resistance value of the ecological source (P_a) and the area of the ecological source (S_a).

3.2 EN optimization

We used the Barrier Mapper module in the Linkage Mapper tool of ArcGISPro v.3.1.0 trial version (Environmental Systems Research Institute (ESRI), Redlands, USA) to simulate current intensity in ecological corridors. Identifying high-resistance areas as ecological barriers provided a scientific basis for determining key restoration areas (Wang et al., 2025b). In addition, we sequentially numbered the ecological nodes to facilitate identification and spatial analysis, following established approaches (Kang et al., 2022; Lü et al., 2022).

Betweenness centrality is a classical metric for assessing the importance of nodes or edges in the process of information transmission within a network (Bröhl and Lehnertz, 2019). In this study, we programmed a method to calculate edge-weighted betweenness and classified the results into five levels using the natural breaks method. Edge betweenness in the top two levels were selected as key corridors, as higher values indicate a stronger intermediary role in ecological flows (Song et al., 2021). For nodes, eigenvector centrality was calculated, and node sizes were proportionally scaled to their eigenvector centrality values to highlight their relative influence within the ENs.

To optimize the ENs, we identified barrier points along key corridors, assessed their restoration potential based on surrounding land use, and accordingly refined the resistance surface (Fig. 3). Following the general approach of previous studies that applied multiple buffer distances to analyze ecological elements (Li et al., 2023; Du et al., 2024), we set a series of buffer distances to quantify the range at which the surrounding dominant land use type of each barrier point stabilized. This allowed us to determine the threshold distance at which the largest number of barrier points' surrounding land reached stability. For barrier points with restoration potential, we used the

dominant land use type within the stability threshold as a reference for restoration and adjusted their resistance values to the mean level of the post-restoration land use type. Restoration was carried out solely through targeted and point-specific resistance adjustments of the surrounding grids for each barrier point, enabling optimization with pixel-level modifications and only minimal alterations to the overall landscape structure. After updating the resistance surface, we reconstructed ecological corridors to evaluate the restoration effects.

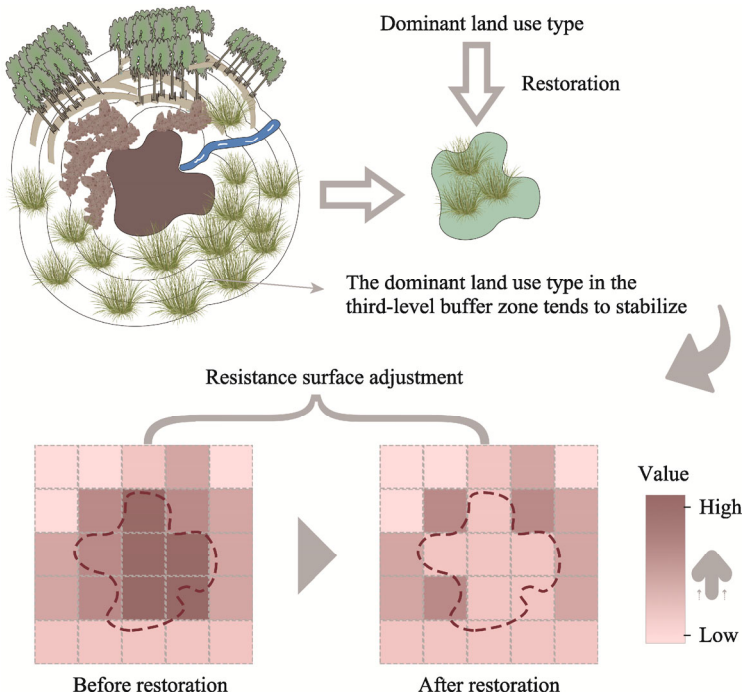

Fig. 3 Schematic diagram of restoration strategy

3.3 EN evaluation

To evaluate the structural robustness of the ENs, we simulated edge removals under random and deliberate attack strategies. Robustness was assessed using two indicators: maximum connected subgraph (MCS) and network efficiency (Ne) (Baggio et al., 2011). Random attacks involved stochastic edge removal to simulate non-specific disturbances, while deliberate attacks removed edges in descending order of betweenness or edge degree. To better account for the weighted nature of the network, following El-Kebir and Klau (2014), we defined MCS as the sum of edge weights in the maximum connected component. Comparing the trends in MCS and Ne across scenarios enabled the identification of network resilience and critical connections. The calculation formulas are as follows:

$$\mathrm{MCS}_t = \frac{\sum_{(c,e)\in E_L^t} w_{ce}}{\sum_{(c,e)\in E_L^0} w_{ce}}, \tag{7}$$

$$Ne_t = \frac{1}{n(n-1)} \sum_{c,e\in V;\ (c\neq e)} \frac{1}{d_{ce}}, \tag{8}$$

where MCS_t is the robustness of the maximum connected subgraph at step t; E_L^t is the edge set of the largest connected component at step t; E_L^0 is the edge set of the initial network before any edge removal; w_{ce} is the weight of edge (c, e); Ne_t is the network efficiency at step t; d_{ce} is the shortest path length between nodes c and e (km); n is the total number of nodes; and V is the set of nodes in the network.

4 Results

4.1 EN construction

4.1.1 Identification of ecological sources

Ecosystem service functions across the study area exhibited significant spatial heterogeneity, and different service types showed distinct spatial distribution patterns (Fig. 4). Food production was high in the eastern and southern plains due to abundant cropland and high agricultural intensity. Raw material production was relatively high in specific forest or grassland areas. High water supply and all regulating service functions were mainly concentrated in the central and northern mountainous areas, where well-preserved vegetation ensured strong regulating functions. In the southern hydrologically active region, water supply and regulating services were particularly prominent. Soil conservation was mainly observed in the northern and eastern regions, reflecting higher landscape stability and vegetation cover. Nutrient cycling and biodiversity maintenance showed medium to high values in well-preserved mountainous areas, indicating strong ecosystem support capacity. Aesthetic landscape services were concentrated around rivers and lakes, with high-value areas mainly in the central and eastern regions. Overall, the total ecosystem service value exhibited a spatial pattern of being high in the central and eastern regions and low in the western region. The spatial differentiation of ecosystem service functions results from the combined influences of natural geography, land use structure, and human activities.

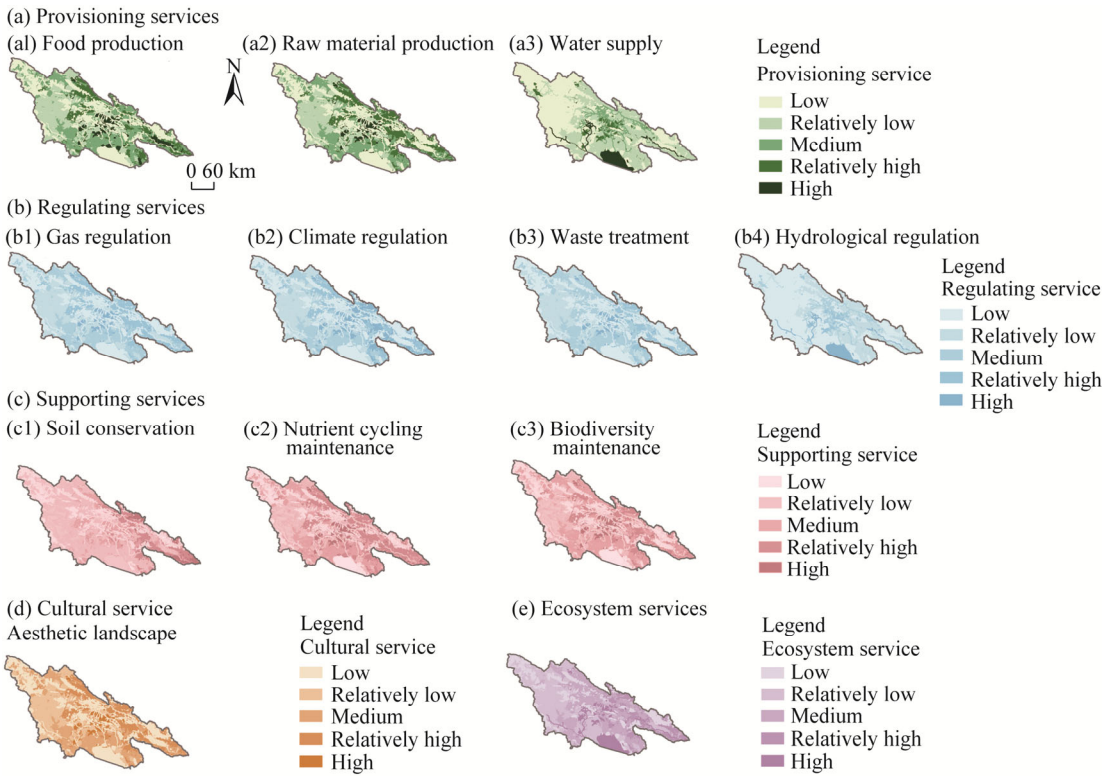

Fig. 4 Spatial distribution of provisioning (a), regulating (b), supporting (c), and cultural (d) service functions and the composite ecosystem service (e) in the southern slope of the Qilian Mountains in 2020. (a1), food production; (a2), raw material production; (a3), water supply; (b1) gas regulation; (b2), climate regulation; (b3), waste treatment; (b4), hydrological regulation; (c1), soil conservation; (c2) nutrient cycling maintenance; (c3) biodiversity maintenance.

To test the rationality of the ecosystem service value equivalent coefficients, we conducted a sensitivity analysis by adjusting the value coefficient of different land use types by ±50.00%. The

results showed that all CS were less than 1.0000, indicating that ecosystem service was inelastic to value coefficient changes, and the adopted coefficients were reasonable, ensuring the robustness and reliability of the estimates (Table 2).

Table 2 Coefficient of sensitivity (CS) of ecosystem service for different land use types

Land use type	Cropland	Forest land	Grassland	Water body	Construction land	Barren land
CS	0.0260	0.0987	0.0595	0.8147	0.0000	0.0013

In the seven types of MSPA landscapes, the core area covered approximately 15,339 km^2, accounting for 25.43% of the total area of the southern slope of the Qilian Mountains (Fig. 5). The study area still retained large-scale natural ecological patches, and these core areas served as important ecological sources for constructing ENs. Apart from the core patches, the remaining landscape types were scattered and limited in area, exhibiting high fragmentation and low connectivity. The edge zones mainly distributed around the core patches, functioned as transitional zones between the core patches and the external environment. The edge zones were the second largest in area after the core zones, and to some extent the edge zones maintained buffering and transitional ecological functions. The bridge zones, though small in area, held significant ecological meaning and could serve as potential corridors within ENs. Therefore, these areas should have been the focus of ecological corridor restoration and optimization. Overall, the landscape structure in the southern slope of the Qilian Mountains still relied on large core patches, but the overall network connectivity was low, and the ecological corridor structure remained incomplete.

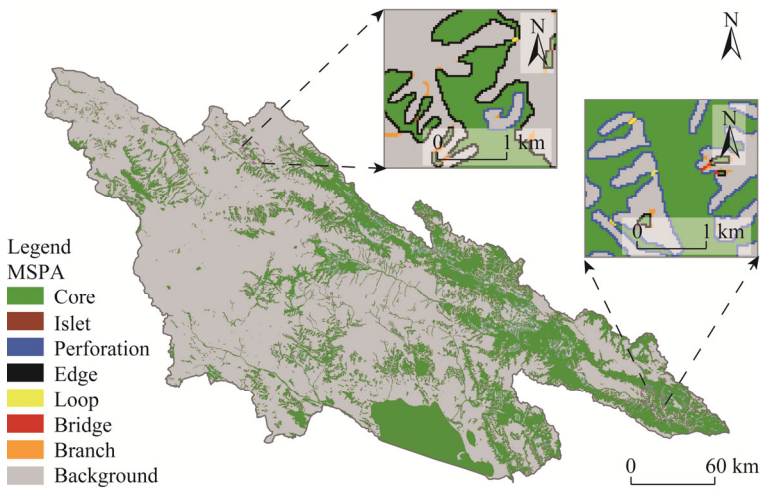

Fig. 5 Spatial distribution of MSPA landscape types in the southern slope of the Qilian Mountains in 2020

We overlaid and analyzed ecosystem service evaluation and MSPA to further identify ecological sources with high ecological function and structural integrity in the region. A total of 494 ecological sources were identified in the southern slope of the Qilian Mountains in this study, covering an area of approximately 9921 km^2, which accounts for 16.45% of the total area (Fig. 6). Overall, ecological sources were primarily concentrated in the northeastern and southeastern parts of the southern slope of the Qilian Mountains, with relatively fewer in the western part. In the northeastern part, ecological sources were densely distributed in a strip shape, mainly due to the continuous distribution of narrow forested areas and high-coverage grasslands. The patches in this area were well connected, and the overall structure was relatively intact. In contrast, the southeastern part mainly consisted of high-coverage grasslands, but due to some fragmentation of vegetation cover, ecological sources were relatively scattered and smaller in size than the northeastern part. Around the Qinghai Lake, a relatively large ecological source patch formed due

to concentrated water bodies and high-quality vegetation, providing strong ecological foundation and high ecosystem service capacity.

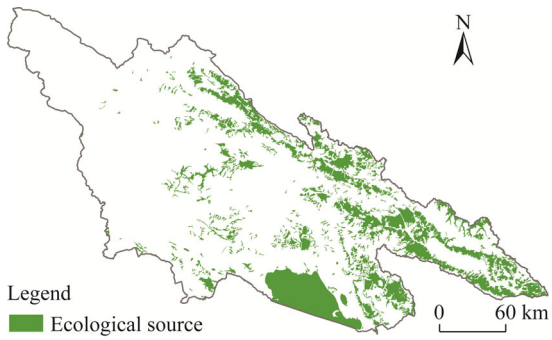

Fig. 6 Spatial distribution of ecological sources in the southern slope of the Qilian Mountains in 2020

4.1.2 Construction of resistance surface

The resistance surface was constructed by overlaying various resistance factors (Fig. 7). The overall resistance surface showed a spatial distribution pattern of "high in the northwest and low in the southeast" (Fig. 8). The northwestern part was characterized by higher elevation and more topographical relief, with primarily barren land and low vegetation coverage. The ecosystem in this area was relatively fragile, resulting in higher ecological resistance and the formation of a distinct high-resistance zone. In contrast, the southeastern part was relatively flat terrain, with landscape dominated by grasslands and water bodies. The high vegetation coverage and ecosystem stability led to lower resistance values, which in turn facilitated the formation of favorable corridors for the migration and diffusion of ecological elements.

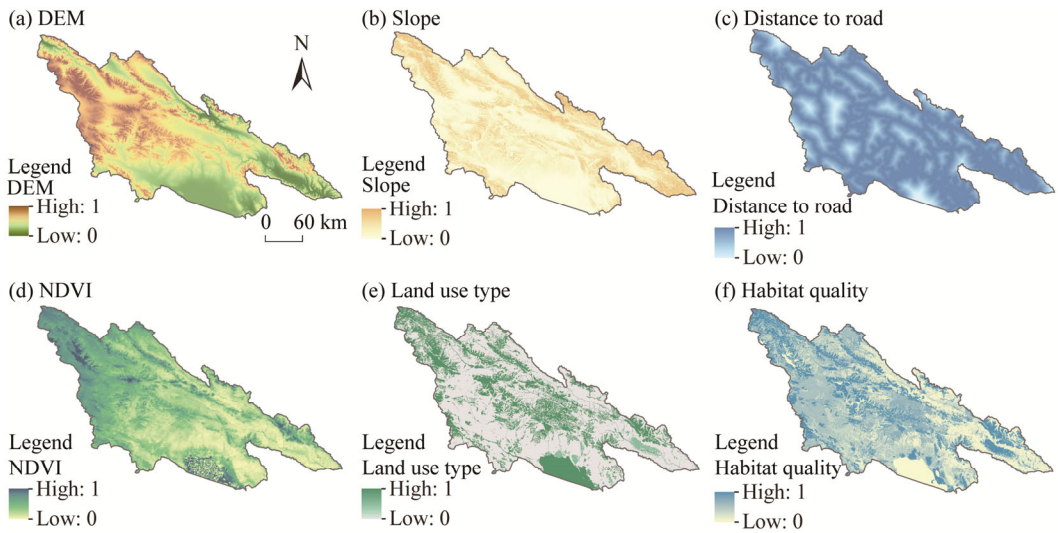

Fig. 7 Spatial distribution of individual resistance factor after uniform weighting process in the southern slope of the Qilian Mountains in 2020. (a), digital elevation model (DEM); (b), slope; (c), distance to road; (d), normalized difference vegetation index (NDVI); (e), land use type; (f), habitat quality.

4.1.3 Extraction of ecological corridors

Using MCR model with ecological sources and the comprehensive resistance surface, we identified 1308 ecological corridors in the southern slope of the Qilian Mountains, with a total length of approximately 7283 km (Fig. 9). Spatially, the resulting ENs exhibited a distinct "dense in the east and sparse in the west" distribution pattern. In the eastern part of the southern slope of the Qilian

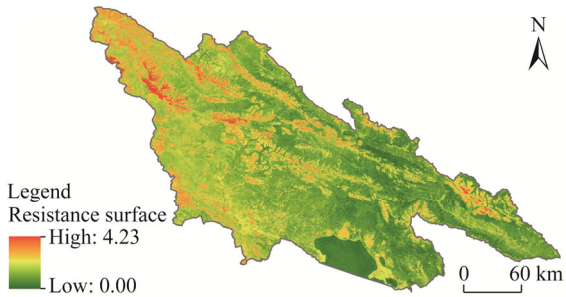

Fig. 8 Spatial distribution of integrated resistance surface of the southern slope of the Qilian Mountains in 2020

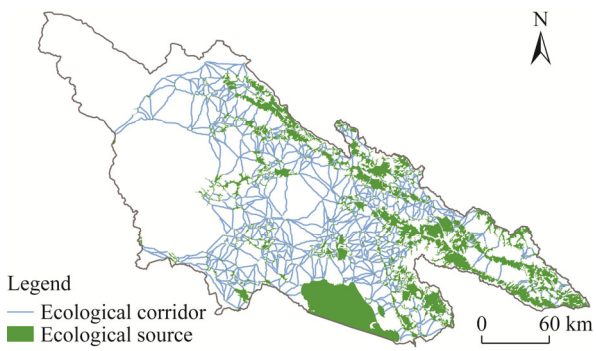

Fig. 9 Spatial distribution of ecological corridors in the southern slope of the Qilian Mountains in 2020

Mountains, ecological sources were dense, and ecological corridors were closely connected, resulting in a relatively complete EN structure with strong spatial connectivity. In contrast, the ENs were noticeably sparse in the western part, where ecological sources were fewer and more scattered. The connections between ecological elements were weak, resulting in a more fragmented network structure.

4.2 EN optimization

4.2.1 Priority classification of ecological corridors based on weighted network edge betweenness

The complex network analysis method, combined with the gravity model, was applied to the ENs to construct a weighted network (Fig. 10). In the complex network, the weight of ecological corridors was represented using different widths, and the betweenness of the network was calculated to determine the priority of ecological corridors. Additionally, the size of the nodes reflected their eigenvector centrality, which indicated the influence of the nodes within the overall network. Representative nodes such as 308, 310, and 312 occupied prominent structural positions in the network. They were concentrated in the northern part of the Qinghai Lake and played a crucial role in the overall network, exhibiting strong connectivity and structural control, which made them key core areas for maintaining network stability. We classified edge betweenness using the natural breaks method to divide ecological corridors into five levels and extracted the first two levels as key corridors to achieve the priority classification of ecological corridors. Overall, key ecological corridors were spatially dispersed, with a relatively higher concentration in the central part, functioning as critical passages for connecting and transitioning multiple ecological paths, and playing a key role in ecological flow. Although the number of ecological sources in the central part was limited, the pronounced intermediary role of corridors in this location rendered these corridors functionally irreplaceable.

4.2.2 Identification of ecological barriers

Using the Barrier Mapper module in Linkage Mapper, we identified 232 ecological barriers, covering an area of approximately 823 km^2 (Fig. 11). These ecological barriers were unevenly distributed across space, with most concentrated in the northwestern and southwestern parts of the

southern slope of the Qilian Mountains. In some regions, they were densely clustered, whereas in others, they appeared more scattered. The ecological barriers were primarily located along key ecological corridors where ecological connectivity between ecological sources was impeded, mainly due to factors such as topographical fragmentation, vegetation degradation, or human disturbances, all of which hindered the effective transfer of ecological processes.

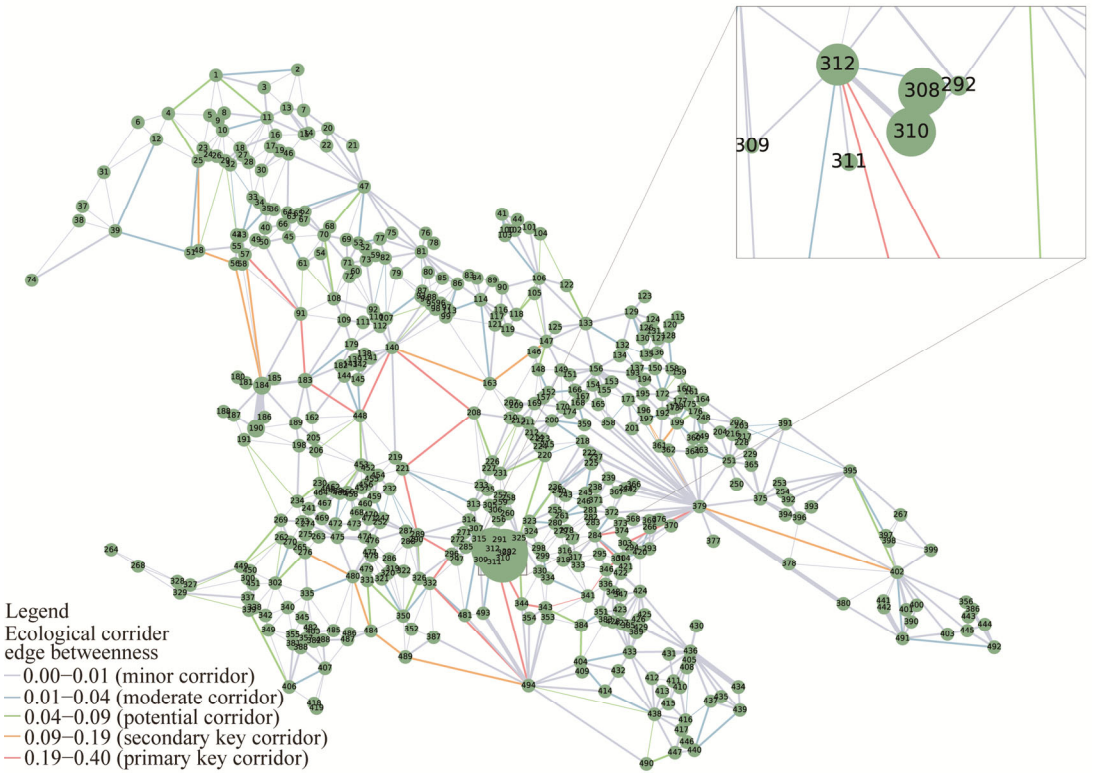

Fig. 10 Weighted complex network and corridor priority classification in the southern slope of the Qilian Mountains in 2020. The size of node reflects the influence of the node within the overall network; the bigger the node is, the higher importance the ecological source is. Numbers in the figure represent the ecological sources identified by this study.

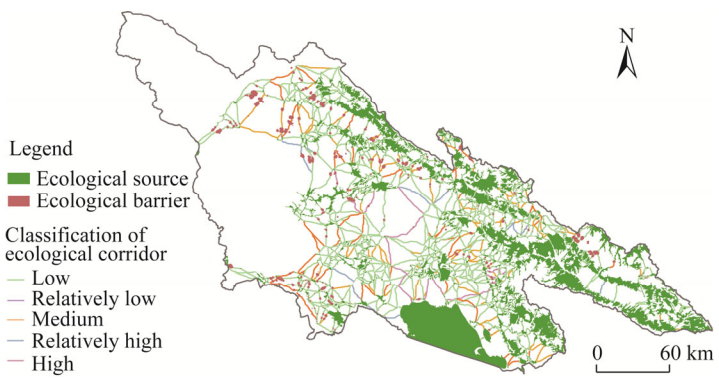

Fig. 11 Spatial distribution of ecological barriers in the southern slope of the Qilian Mountains in 2020

4.2.3 Ecological restoration based on barriers along key ecological corridors

A total of 99 barrier points were identified on key ecological corridors following the prioritization of ecological corridors (Fig. 12). In terms of spatial distribution, large barrier points were primarily concentrated in key ecological corridor areas in the northwestern part of the southern slope of the

Qilian Mountains, where ecological connectivity was significantly obstructed. Some of these ecological barriers were located in high-altitude mountainous areas characterized by complex terrain and high restoration difficulty. In addition, several barrier points were heavily impacted by human activities, for instance, Barrier Points 85 and 92 were situated within cropland, Barrier Point 87 lay at the junction of cropland and a river, Barrier Points 77 and 93 were distributed along major transportation routes, and Barrier Point 81 was located within a densely populated residential area. Although these barrier points were spatially dispersed, they generally posed considerable challenges for restoration and imposed substantial constraints on the continuity of key ecological corridors. Ultimately, based on the specific conditions of each barrier point, we identified 51 priority restoration sites.

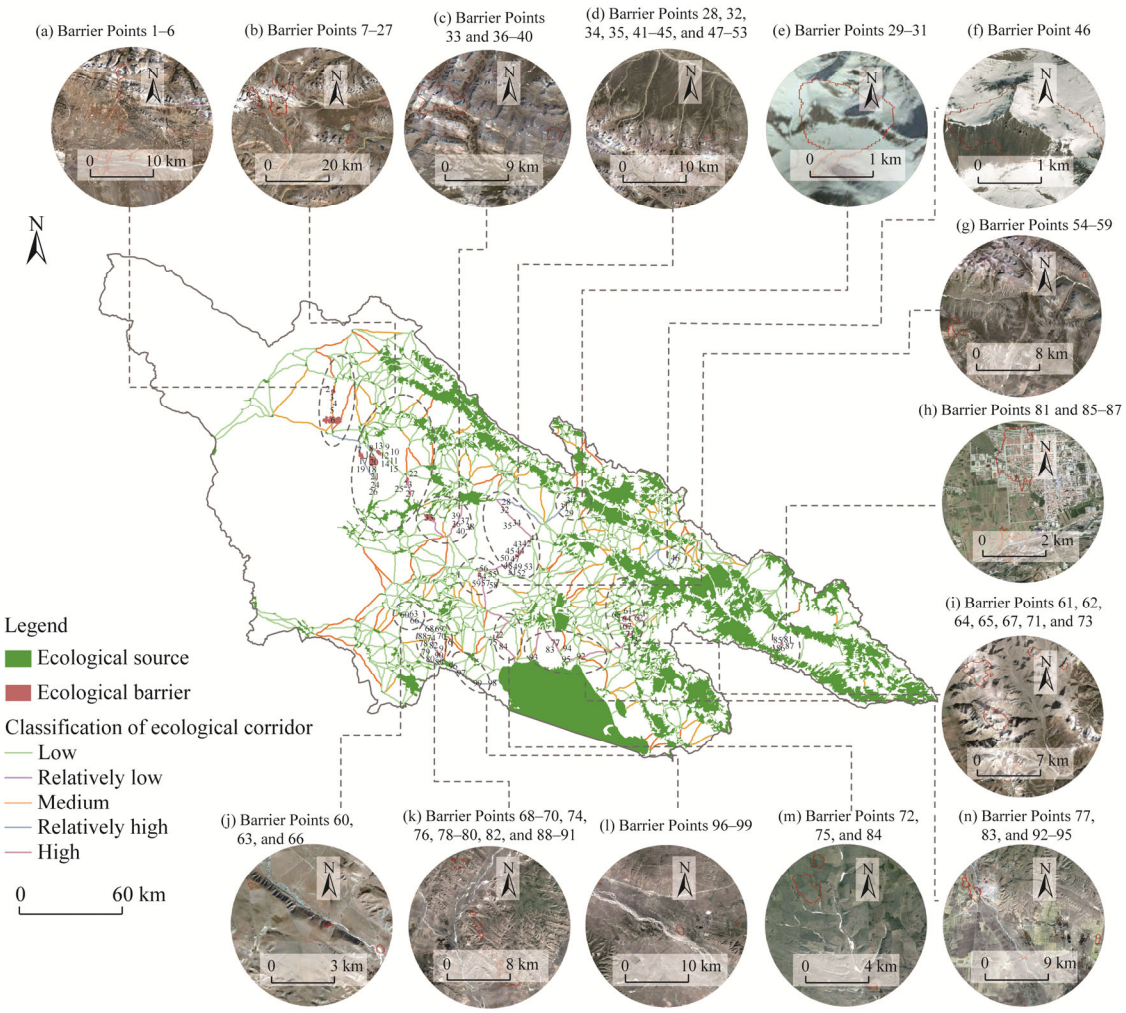

Fig. 12 Spatial distribution of barrier points on the key ecological corridors in the southern slope of the Qilian Mountains in 2020. (a), Barrier Points 1–6; (b), Barrier Points 7–27; (c), Barrier Points 33 and 36–40; (d), Barrier Points 28, 32, 34, 35, 41–45, and 47–53; (e), Barrier Points 29–31; (f), Barrier Point 46; (g), Barrier Points 54–59; (h), Barrier Points 81 and 85–87; (i), Barrier Points 61, 62, 64, 65, 67, 71, and 73; (j), Barrier Points 60, 63, and 66; (k), Barrier Points 68–70, 74, 76, 78–80, 82, and 88–91; (l), Barrier Points 96–99; (m), Barrier Points 72, 75, and 84; (n), Barrier Points 77, 83, and 92–95.

To characterize the surrounding land use patterns of barrier points and assess their potential transformation directions, we established buffer zones at 500, 1000, 1500, 2000, and 2500 m. For each distance, the dominant land use types of priority restoration barrier points were identified, and the number of barrier points reaching a stable state under varying buffer conditions was recorded

(Fig. 13). The results indicated that when the buffer radius reached 2000 m, the dominant land use types stabilized, and changes in spatial heterogeneity became significantly less pronounced. Therefore, based on the dominant land use types within 2000 m buffer zone, we investigated the transformation potential of barrier points. Considering the ecological resistance characteristics of different land use types, we simulated targeted restoration by adjusting the resistance values of the barrier points to the average resistance values of their potential target land use types. This approach effectively optimized the local resistance surface without significantly altering the regional ecological pattern, thereby reducing ecological resistance at critical barrier points and providing a feasible pathway to enhance connectivity and overall restoration efficiency within the ENs.

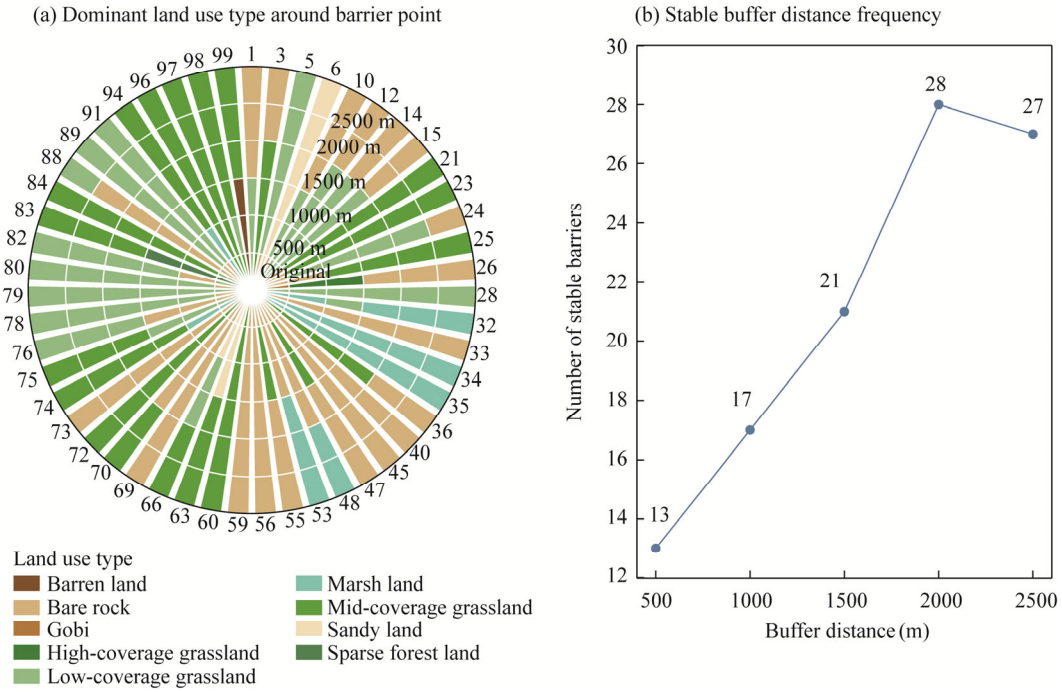

Fig. 13 Integrated visualization of land use types (a) and stability of selected barrier points as restoration sites across different buffer distances (b) in the southern slope of the Qilian Mountains in 2020

The overall spatial pattern of the optimized resistance surface after ecological restoration remained consistent with that before restoration, still exhibiting a general distribution of "high in the northwest, low in the southeast" (Fig. 14). However, through the rational transformation of land use types and the adjustment of resistance values around the priority restoration barrier points, resistance values in some local areas significantly decreased. In particular, the discontinuity of the resistance surface in certain originally high-resistance areas was alleviated to some extent, leading to improved ecological connectivity. Although the overall resistance level of the southern slope of the Qilian Mountains did not show a marked decline, the average resistance value across all restored barrier areas decreased from 2.36 to 1.56. For example, the resistance value near Barrier Point 75 decreased from 2.03 to 1.58, while that around Barrier Point 91 decreased from 2.10 to 1.68, both showing substantial local reductions, confirming the effectiveness of the optimization in alleviating local ecological resistance and enhancing connectivity.

4.2.4 Construction of the optimized ENs

After optimization of the resistance surface following ecological restoration, a total of 1319 ecological corridors were identified, with an overall length of approximately 8426 km (Fig. 15). Compared with the pre-restoration state, the number of ecological corridors increased from 1308 to 1319, resulting in a net gain of 11 ecological corridors. Among the optimized ENs, 25 original

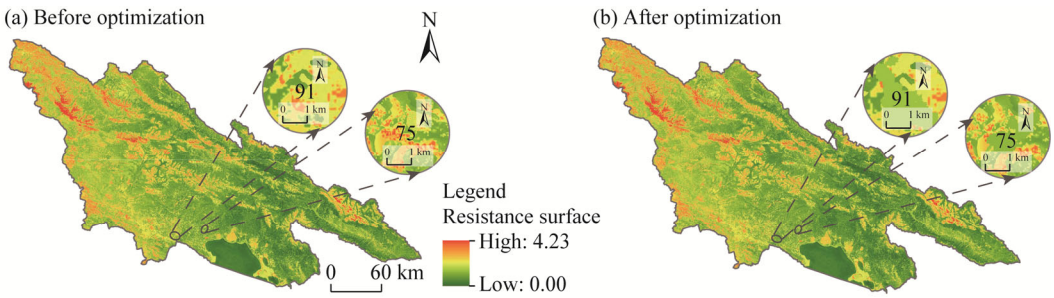

Fig. 14 Spatial distribution of the ecological resistance surface before (a) and after optimization (b) in the southern slope of the Qilian Mountains in 2020

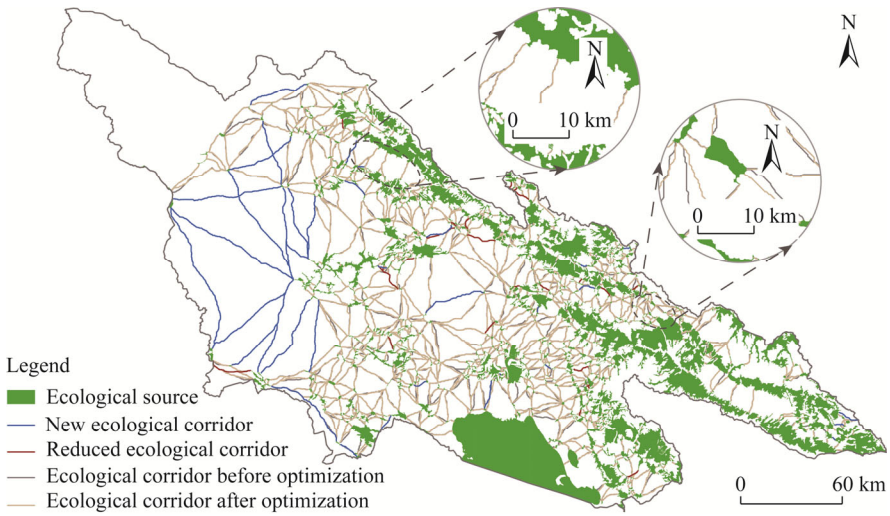

Fig. 15 Spatial distribution of ecological corridors after optimization

ecological corridors were removed, and 36 new ones were added. This change primarily reflected the elimination of redundant or inefficient paths, while the restoration of barrier points and improved connectivity among ecological sources led to the addition of more reasonable and efficient ecological corridors, thereby enhancing the overall connectivity and stability of the ENs. The total ecological corridor length increased by approximately 1143 km, indicating that the optimized resistance environment provided more feasible pathways for ecological connectivity. In terms of spatial distribution, the optimized ecological corridors largely maintained the original pattern, characterized by a "sparse in the west and dense in the east" layout. However, ecological corridor density in the west increased significantly. In some areas, overlaps occurred between original and newly added ecological corridors, while in others, clear shifts in local pathways were observed, reflecting localized adjustments made during the optimization process. Notably, the emergence of relatively long corridors in the northwestern part can be explained by ecological processes. The restoration of barrier points improved local ecological quality, thereby eliminating previous obstructions to species movement and enhancing habitat suitability. As a result, new feasible connections emerged among scattered ecological sources. Given that ecological sources in the western region were relatively sparse and widely distributed, the improvement in connectivity was manifested as longer ecological corridors, which remain within the dispersal capacities of target species and thus represent ecologically reasonable pathways.

4.3 Evaluation of EN optimization effects

To quantify the structural stability and disturbance resistance of the ENs before and after optimization, we simulated the robustness changes of the ENs under edge attack based on the two metrics of MCS and Ne. The robustness degradation curves were then plotted (Fig. 16).

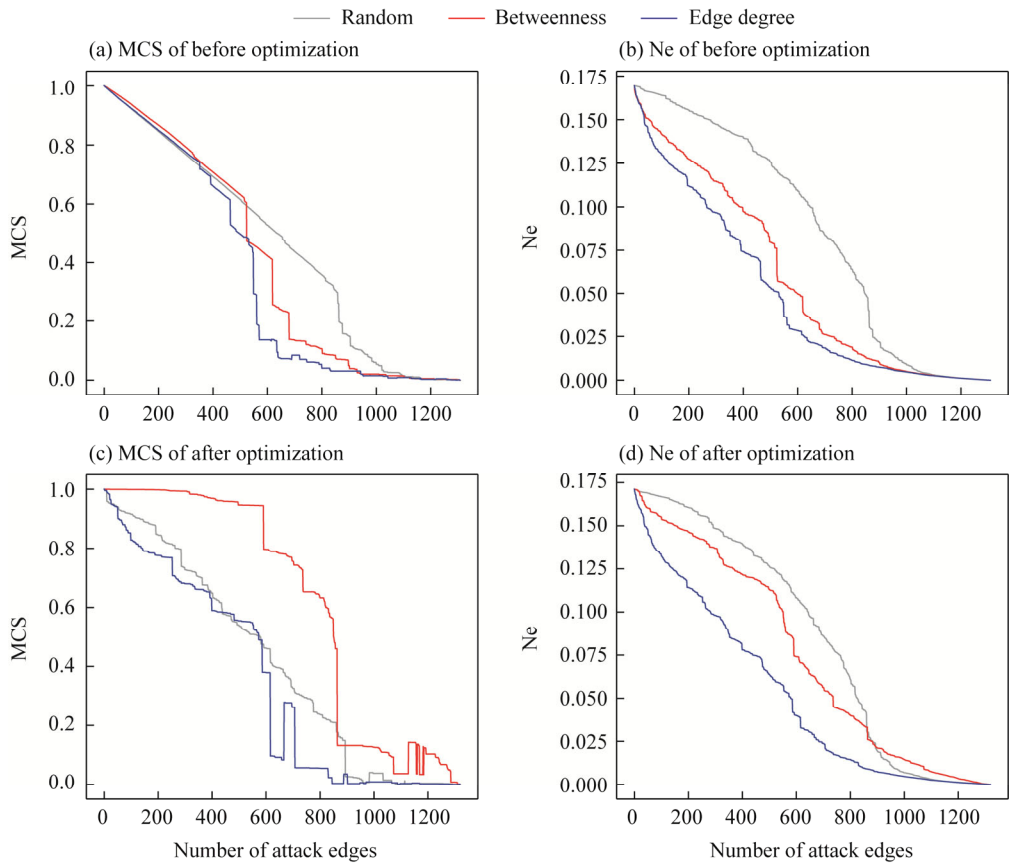

Fig. 16 Changes in robustness of ENs before (a and b) and after (c and d) optimization under different attack methods in the southern slope of the Qilian Mountains in 2020. MCS, maximum connected subgraph; Ne, network efficiency.

Overall, the network structure exhibited varying degrees of degradation under all three types of attacks, but the extent of the impact differed significantly. Under edge degree-based attacks, both the MCS and Ne of the ENs declined most rapidly, indicating that edges with high connectivity played a critical role in maintaining overall connectivity, and their failure quickly weakened the structural stability of the network. In contrast, betweenness attacks had the second most significant destructive effect, while random attacks caused the slowest degradation, with the curves showing a more gradual decline.

After optimization, the network's robustness generally improved. Regarding structural indicators before the attack, Ne increased from 0.169 to 0.171, suggesting a slight but noticeable improvement in the network's connectivity and functional transmission capacity in initial state. During the simulated attacks, the optimized network exhibited a slower decline in both MCS and Ne curves at most stages. In particular, the degradation trend under betweenness attacks was significantly alleviated, highlighting the more pronounced effect of optimization. Although the indicators under random attacks showed little difference before and after optimization, the decline curve became smoother, reflecting enhanced local resilience. Under edge degree-based attacks, the optimization effect was less prominent; however, the divergence in the curves became apparent around the 600th attack edge, indicating that the restoration measures still maintained relatively high network integrity during certain stages. Notably, MCS displayed brief rebounds at certain stages, reflecting the emergence of secondary subgraphs with high edge weights temporarily becoming the largest connected component when the original maximal subgraph fragmented.

5 Discussion

5.1 EN optimization

In this study, the ENs constructed for the southern slope of the Qilian Mountains in 2020 exhibited a typical spatial pattern of "dense in the east and sparse in the west". This pattern was consistent with previous research on ENs in the Qilian Mountains area (Dong et al., 2024; Gao et al., 2024a), validating the reasonableness of the identified ecological sources and corridors. To further analyze the internal structural characteristics and operational mechanisms of the ENs, we abstracted the ENs as a weighted complex network model. By introducing a gravity-based weighting approach (Gao et al., 2023), we quantified the interaction intensity between ecological sources, allowing the "ecological flow" carried by different ecological corridors to vary. This approach more accurately reflects ecological processes, such as species migration and energy exchange, in real ecosystems, where these processes do not occur equally across all pathways (Wu et al., 2024; Zou et al., 2024). The weighted complex network model not only enhances the scientific rigor of the study but also provides foundational support for subsequent network analysis and optimization. Given the resource costs and feasibility of ecological restoration, we did not apply repairs to all ecological barriers uniformly (Beltrão et al., 2024). Instead, we identified key ecological corridors with high betweenness in the overall network and prioritized the restoration of ecological barriers located on these ecological corridors. This approach allows for significant improvements in overall network connectivity at a relatively low cost, offering higher cost-effectiveness and operational value.

Unlike existing studies that often adopt strategies such as "adding new ecological corridors or sources", our approach focused on a different direction. For example, Wang et al. (2025b) strengthened connections by constructing ecological corridors between ecological sources with low edge degree and low betweenness. Similarly, Wang et al. (2022a) and Sun et al. (2024b) improved overall connectivity by introducing new ecological sources. While these methods enhanced network robustness and ecological process accessibility to some extent, they inevitably increased connectivity as a natural result of structurally adding nodes and edges to the network. However, in certain ecologically sensitive areas or regions where the ecological pattern is already stable, indiscriminately adding ecological sources or corridors not only faces high land regulation and ecological restoration costs but may also lead to new land use conflicts, making sustainable ecological management difficult to achieve (Li et al., 2022; Han et al., 2024). Therefore, we proposed a prudent optimization approach that restores the dominant land use types immediately surrounding key ecological barriers to reduce ecological resistance, achieving a "soft optimization" of the ENs without adding new nodes or edges while preserving the original landscape pattern. Compared with large-scale structural reorganization, this localized strategy confines interventions to obstructed zones, thereby minimizing land-cover conversions, preserving the high-quality environmental background around ecological barriers, and reducing restoration and regulatory costs (McRae et al., 2012). This approach achieves a relatively minimal scale and cost of restoration while delivering substantial gains in ecological connectivity. The observed improvement in local habitat connectivity following ecological barrier restoration demonstrates the tangible ecological benefits of this relatively minimal and targeted optimization.

In addition, we fully considered the spatial location and practical intervention difficulty of the barrier points in restoration strategy. For instance, some barrier points are located in high-altitude snow-capped mountain areas, where ecological restoration is extremely difficult due to terrain and climatic constraints. Other barrier points are situated on transportation roads or rivers, with strong rigid constraints that are hard to alter. Furthermore, some barrier points are located in densely populated residential areas, where ecological restoration would require significant social coordination and relocation costs. Considering these practical constraints, we didn't adopt a unified restoration approach. Instead, we focused on "repairability" and only implemented restoration strategies for barrier points with higher operational feasibility. At the same time, to ensure the scientific and practical nature of the restoration, we did not simply convert barrier land use types into the highest ecological value land use types, such as forests. Instead, we determined the

conversion based on the dominant land use types within the buffer zone of the barrier points. For example, if the surrounding area is mainly grassland, the priority would be to convert it to a grassland type. This tailored restoration approach respects the existing land use pattern while enhancing the accessibility of regional ecological processes, providing a practical path for precise ENs management.

5.2 EN optimization effects

Contrary to initial expectations, the optimization of the ENs did not simply result in an increase in the number of ecological corridors. Instead, it was accompanied by a reduction in some of the original ecological corridors and the creation of new ones, with 25 existing ecological corridors being removed and 36 new ecological corridors being added. This phenomenon suggests that evaluating the effectiveness of optimization solely based on changes in the number of ecological corridors is insufficient; the increase in the total length of ecological corridors more accurately reflects the improvement in ecological connectivity potential (Gilbert-Norton et al., 2010; Li et al., 2021). These ecological corridors served as the primary pathways for ecological flows and information exchange between habitats, and changes in their number and length directly facilitated species migration and other ecological processes. From a spatial perspective, the optimized corridors did not strictly follow the original paths. Although most of the corridors remained largely consistent with their pre-optimization orientation, there were still local differences. On one hand, these local variations is attributed to the inherent characteristics of the circuit theory used in the simulation process, where even when connecting the same ecological sources, the ecological corridors generated before and after optimization cannot completely overlap. On the other hand, in certain areas, the restoration of barrier points reduces local resistance, allowing circuit theory model to identify new paths with better connectivity during the optimization process, leading to noticeable ecological corridor shifts. This shift not only expands the feasible pathways for ecological flow, but also demonstrates the enhanced adaptability and structural flexibility of the ENs under local restoration strategies. As a result, the network's overall connectivity and ecological functional stability are further improved.

To more accurately characterize the spatial transmission characteristics of ecological processes, we introduced weighted cost distance as the basis for connectivity assessment in EN construction, differing from traditional network models that rely on physical distance or unweighted connections (Xu et al., 2024). This approach is more in line with the heterogeneous nature of ecological flow in real-world ecosystems. On this basis, the connectivity and robustness of the network before and after optimization were evaluated using MCS and Ne indicators. Although the absolute values of these indicators showed small improvements (Ne increased from 0.169 to 0.171), MCS and Ne curves for the optimized network exhibited a significant slowdown in the downward trend during simulated edge degree-based attacks, with particularly improved stability under betweenness attacks. Edges with high betweenness carry more ecological interactions between ecological sources, reflecting their key role in maintaining functional connectivity (Gilbert-Norton et al., 2010; Luo and Wu, 2021). The enhanced stability of the optimized network under betweenness attacks demonstrates that these critical paths effectively support ecological processes, ensuring the resilience and functional integrity of the network after optimization.

Notably, the optimized network exhibited a "fluctuating rebound" phenomenon in MCS during the attack process, where the maximum connected subgraph did not continuously decline at certain stages, but rather briefly increased. Rather than relying on node count, the MCS metric in this study was constructed from the total edge weight of the connected subgraph to capture the intrinsic weighted characteristics of the network. While the original maximum subgraph break apart and its weight decreases, other more compact secondary connected components with higher edge weights but fewer nodes might rise to become the new maximum connected subgraph, leading to a temporary increase. This phenomenon reflects the potential redundancy in the optimized network structure and the alternative connectivity functions, indicating that the network has stronger resilience after key pathways are damaged. This phenomenon further demonstrates the effectiveness of the optimization strategy: the optimized EN possesses enhance functional transfer

ability and elasticity, enabling it to quickly hand over connectivity functions to secondary structures after key connections are disrupted, thereby maintaining overall system connectivity and ecological functional stability.

5.3 Limitations and prospects

We resampled 1 km resolution data (e.g., NPP and precipitation) to 30 m to ensure data consistency. Given the constraints of data availability and timeliness, this resampling may have some impact on the accuracy of ecosystem service adjustments; however, the overall pattern remains generally consistent with the actual ecological conditions of the study area. Although the gravity model allows for differentiated ecological corridor weighting and better reflects spatial ecological processes, the weighting still relies on objective indicators like source area and resistance distance, failing to fully capture real species migration dynamics. Incorporating field-tracked migration data could improve realism but is limited by high costs and data scarcity. Additionally, robustness analysis focused on static structural responses, overlooking the adaptive and redundant properties of real ecosystems. Future studies should consider dynamic models to better simulate ENs' responses and enhance the robustness of optimization strategies. The study focused on localized optimization, whereas quantitative comparisons with large-scale structural reorganization remain lacking; future work could assess their relative efficiency in enhancing ecological connectivity and reducing restoration costs.

6 Conclusions

This study adopted an "ecological source–resistance surface–corridor" framework, applied circuit theory to identify ecological barriers, and integrated a weighted complex network approach to locate ecological barriers along key ecological corridors. Multi-level buffer zones guided localized restoration of the ecological barrier points with restoration potential, after which the EN was reconstructed and its optimization was evaluated. The ENs showed evident spatial differentiation, with ecological sources mainly concentrated in the northeastern and southeastern parts of the south slope of the Qilian Mountains, while corridors were denser in the eastern part and sparser in the western part. Using a 2000-m buffer as the restoration reference and considering each ecological barrier's practical restoration potential, we selected 51 ecological barrier points along key ecological corridors for localized restoration. After resistance adjustment and network reconstruction, the newly added ecological corridors were mainly concentrated in the western part with previously weak connectivity. Under simulated attack scenarios, both the decline rates of MCS and Ne decreased more slowly. These results demonstrate that localized restoration of key ecological barriers significantly enhances ecological connectivity and structural robustness without altering the overall landscape pattern, providing practical guidance for ecological restoration in semi-arid mountain areas.

Conflict of interest

The authors declare that they have no known competing financial interests or personal relationships that could have appeared to influence the work reported in this paper.

Acknowledgements

This work was supported by the Sichuan Science and Technology Program (2022JDJQ0015), the Major Research and Development and Achievement Transformation Projects of Qinghai Province, China (2022-QY-224), and the National Natural Science Foundation of China (42471225).

Author contributions

Conceptualization: PAN Yilu; Data curation: YANG Xia; Methodology: PAN Yilu; Formal analysis: PAN Yilu; Writing - original draft preparation: PAN Yilu; Writing - review and editing: PAN Hongyi; Funding acquisition:

PAN Hongyi; Resources: PAN Hongyi; Supervision: PAN Hongyi, ZHANG Wen; Visualization: YANG Xia, FANG Yuxuan. All authors approved the manuscript.

References

Albert R, Barabási A L. 2002. Statistical mechanics of complex networks. Reviews of Modern Physics, 74: 47, doi: 10.1103/RevModPhys.74.47.

Baggio J A, Salau K, Janssen M A, et al. 2011. Landscape connectivity and predator–prey population dynamics. Landscape Ecology, 26(1): 33–45.

Barrat A, Barthélemy M, Pastor-Satorras R, et al. 2004. The architecture of complex weighted networks. Proceedings of the National Academy of Sciences of the United States of America, 101(11): 3747–3752.

Beltrão M G, Gonçalves C F, Brancalion P H S, et al. 2024. Priority areas and implementation of ecological corridor through forest restoration to safeguard biodiversity. Scientific Reports, 14(1): 30837, doi: 10.1038/s41598-024-81483-y.

Bröhl T, Lehnertz K. 2019. Centrality-based identification of important edges in complex networks. Chaos: An Interdisciplinary Journal of Nonlinear Science, 29(3): 033115, doi: 10.1063/1.5081098.

Cao W J, Jia G X, Yang Q K, et al. 2024. Construction of ecological network and its temporal and spatial evolution characteristics: A case study of Ulanqab. Ecological Indicators, 166: 112344, doi: 10.1016/j.ecolind.2024.112344.

Chen F Y, Luo Q L, Zhu Z B. 2025a. Integrating static and dynamic analyses in a spatial management framework to enhance ecological networks connectivity in the context of rapid urbanization. Ecological Modelling, 501: 111022, doi: 10.1016/j.ecolmodel.2025.111022.

Chen J, Wang S S, Zou Y T. 2022. Construction of an ecological security pattern based on ecosystem sensitivity and the importance of ecological services: A case study of the Guanzhong Plain Urban Agglomeration, China. Ecological Indicators, 136: 108688, doi: 10.1016/j.ecolind.2022.108688.

Chen X Y, Zhu B C, Li T S, et al. 2025b. Ecological risk networks: A network structure model for simulating negative ecological linkages among ecologically sensitive areas. International Journal of Disaster Risk Reduction, 119: 105316, doi: 10.1016/j.ijdrr.2025.105316.

Costa A, Martín González A M, Guizien K, et al. 2019. Ecological networks: Pursuing the shortest path, however narrow and crooked. Scientific Reports, 9(1): 17826, doi: 10.1038/s41598-019-54206-x.

Dong C, Yu H Y, Qian X L, et al. 2024. Enhancing ecological connectivity in the Qilian Mountains: Integrating GCA and optimized MST models for ecological corridor construction. Ecological Indicators, 166: 112525, doi: 10.1016/j.ecolind.2024.112525.

Du S, Xu D Z, Sun F Y, et al. 2024. Identification of key areas for territorial ecological restoration: Focusing on ecological security and restoration potential. Frontiers in Environmental Science, 12: 1463683, doi: 10.3389/fenvs.2024.1463683.

El-Kebir M, Klau G W. 2014. Solving the maximum-weight connected subgraph problem to optimality. arXiv preprint arXiv: 1409.5308, doi: 10.48550/arXiv.1409.5308.

Estrada E, Bodin Ö. 2008. Using network centrality measures to manage landscape connectivity. Ecological Applications, 18(7): 1810–1825.

Fenu G, Pau P L. 2018. Connectivity analysis of ecological landscape networks by cut node ranking. Applied Network Science, 3(1): 22, doi: 10.1007/s41109-018-0085-0.

Fu H X, Zhang T, Wang J G. 2024. Evaluating suitability of development and construction with of minimum cumulative resistance model for a mountain scenic area in Jinyun Xiandu, China. Ecological Engineering, 202: 107240, doi: 10.1016/j.ecoleng.2024.107240.

Fu J X, Cao G C, Guo W J. 2020. Land use change and its driving force on the southern slope of Qilian Mountains from 1980 to 2018. Chinese Journal of Applied Ecology, 31(8): 2699–2709. (in Chinese)

Gao C, Pan H Y, Wang M C, et al. 2023. Identifying priority areas for ecological conservation and restoration based on circuit theory and dynamic weighted complex network: A case study of the Sichuan Basin. Ecological Indicators, 155: 111064, doi: 10.1016/j.ecolind.2023.111064.

Gao C, Wang M C, Yuan M, et al. 2024a. Incorporating seasonality, predictability, and modularity into the optimization of biodiversity conservation for ecological networks. Journal of Environmental Management, 370: 122473, doi: 10.1016/j.jenvman.2024.122473.

Gao J, Gong J, Li Y, et al. 2024b. Ecological network assessment in dynamic landscapes: Multi-scenario simulation and conservation priority analysis. Land Use Policy, 139: 107059, doi: 10.1016/j.landusepol.2024.107059.

Gao X, Liang X Y, Guo Z Y, et al. 2024c. The analysis of ecological network characteristics of Baiyangdian Basin in China using the complex network theory. Ecological Indicators, 167: 112650, doi: 10.1016/j.ecolind.2024.112650.

Gilbert-Norton L, Wilson R, Stevens J R, et al. 2010. A meta-analytic review of corridor effectiveness. Conservation Biology, 24(3): 660–668.

Gong W F, Liu T D, Duan X Y, et al. 2022. Estimating the soil erosion response to land-use land-cover change using GIS-based RUSLE and remote sensing: A case study of Miyun Reservoir, North China. Water, 14(5): 742, doi: 10.3390/w14050742.

Gu T, Tong Y W, Wang S Y, et al. 2024. Identifying the priority areas for ecological protection considering ecological connectivity and ecosystem integrity: A case study of Xianyang City, China. Ecological Indicators, 163: 112102, doi: 10.1016/j.ecolind.2024.112102.

Guan J J, Hu J M, Li B N. 2024. How to restore ecological impacts from wind energy? An assessment of Zhongying Wind Farm through MSPA-MCR model and circuit theory. Ecological Indicators, 163: 112149, doi: 10.1016/j.ecolind.2024.112149.

Guo P F, Zhang F F, Wang H Y. 2022. The response of ecosystem service value to land use change in the middle and lower Yellow River: A case study of the Henan section. Ecological Indicators, 140: 109019, doi: 10.1016/j.ecolind.2022.109019.

Guo Z Y, Zhu C X, Fan X, et al. 2025. Analysis of ecological network evolution in an ecological restoration area with the MSPA-MCR model: A case study from Ningwu County, China. Ecological Indicators, 170: 113067, doi: 10.1016/j.ecolind.2024.113067.

Han P Y, Xiong H J, Hu H Z, et al. 2024. Integrating risk-conflict assessment for constructing and optimizing ecological security patterns of polder landscape in the urban-rural fringe. Ecological Indicators, 166: 112256, doi: 10.1016/j.ecolind.2024.112256.

He J, Wang N L, Chen A, et al. 2019. Glacier changes in the Qilian Mountains, Northwest China, between the 1960s and 2015. Water, 11(3): 623, doi: 10.3390/w11030623.

He Y M, Pan H Y, Wang R S, et al. 2023. Research on the cumulative effect of multiscale ecological compensation in river basins: A case study of the Minjiang River Basin, China. Ecological Indicators, 154: 110605, doi: 10.1016/j.ecolind.2023.110605.

Hong W Y, Liu Y K, Wang W X, et al. 2025. Optimization model for urban ecological network connectivity considering geospatial constraints. Geo-spatial Information Science, 28(4): 1866–1879.

Huang L Y, Wang J, Fang Y, et al. 2021. An integrated approach towards spatial identification of restored and conserved priority areas of ecological network for implementation planning in metropolitan region. Sustainable Cities and Society, 69: 102865, doi: 10.1016/j.scs.2021.102865.

Huang X Y, Xiu L N, Lu Z X, et al. 2025. Ecological networks construction and optimization in the Longdong Loess Plateau: The advantages of self-organizing map and complex networks. Ecological Indicators, 170: 113138, doi: 10.1016/j.ecolind.2025.113138.

Jiang H, Peng J, Zhao Y N, et al. 2022. Zoning for ecosystem restoration based on ecological network in mountainous region. Ecological Indicators, 142: 109138, doi: 10.1016/j.ecolind.2022.109138.

Jiang H, Peng J, Liu M L, et al. 2024a. Integrating patch stability and network connectivity to optimize ecological security pattern. Landscape Ecology, 39(3): 54, doi: 10.1007/s10980-024-01852-w.

Jiang J W, Cai J W, Peng R, et al. 2024b. Establishment and optimization of urban ecological network based on ecological regulation services aiming at stability and connectivity. Ecological Indicators, 165: 112217, doi: 10.1016/j.ecolind.2024.112217.

Kang J M, Li C L, Li M R, et al. 2022. Identifying priority areas for conservation in the lower Yellow River Basin from an ecological network perspective. Ecosystem Health and Sustainability, 8(1): 2105751, doi: 10.1080/20964129.2022.2105751.

Li D B, Clements C F, Shan I L G, et al. 2021. Corridor quality affects net movement, size of dispersers, and population growth in experimental microcosms. Oecologia, 195(2): 547–556.

Li J C, Shan R, Yuan W H. 2023. Constructing the landscape ecological security pattern in the Dawen River Basin in China: A framework based on the circuit principle. International Journal of Environmental Research and Public Health, 20(6): 5181, doi: 10.3390/ijerph20065181.

Li P X, Cao H, Sun W, et al. 2022. Quantitative evaluation of the rebuilding costs of ecological corridors in a highly urbanized city: The perspective of land use adjustment. Ecological Indicators, 141: 109130, doi: 10.1016/j.ecolind.2022.109130.

Liang G F, Niu H B, Li Y. 2023. A multi-species approach for protected areas ecological network construction based on landscape connectivity. Global Ecology and Conservation, 46: e02569, doi: 10.1016/j.gecco.2023.e02569.

Liu J, Chen J J, Yang Y P, et al. 2023a. Construction and optimization of an ecological network in the Yellow River source region based on MSPA and MCR modelling. International Journal of Environmental Research and Public Health, 20(4): 3724, doi: 10.3390/ijerph20043724.

Liu X, Han Y, Li Y H, et al. 2024. Construction of ecological network in Daihai Basin based on ecological security pattern and ecological service accessibility. Ecological Frontiers, 44(6): 1224–1231.

Liu X Y, Su Y, Li Z G, et al. 2023b. Constructing ecological security patterns based on ecosystem services trade-offs and ecological sensitivity: A case study of Shenzhen Metropolitan Area, China. Ecological Indicators, 154: 110626, doi: 10.1016/j.ecolind.2023.110626.

Lü L, Zhang S H, Zhu J, et al. 2022. Ecological restoration strategies for mountainous cities based on ecological security patterns and circuit theory: A case of central urban areas in Chongqing, China. International Journal of Environmental Research Public Health, 19(24): 16505, doi: 10.3390/ijerph192416505.

Lu Y C, Huang D, Tong Z M, et al. 2024. A conceptual framework for constructing and evaluating directed ecological networks: Evidence from Wuhan Metropolitan Area, China. Environmental Impact Assessment Review, 106: 107464, doi: 10.1016/j.eiar.2024.107464.

Luo J L, Zhu L, Fu H. 2024. Construction of wetland ecological network based on MSPA-conefor-MCR: A case study of Haikou City. Ecological Indicators, 166: 112329, doi: 10.1016/j.ecolind.2024.112329.

Luo Y H, Wu J S. 2021. Linking the minimum spanning tree and edge betweenness to understand arterial corridors in an ecological network. Landscape Ecology, 36(5): 1549–1565.

McRae B H, Hall S A, Beier P, et al. 2012. Where to restore ecological connectivity? Detecting barriers and quantifying restoration benefits. PLoS ONE, 7(12): e52604, doi: 10.1371/journal.pone.0052604.

Nie H R, Zhao Y, Zhu J, et al. 2024. Ecological security pattern construction in typical oasis area based on ant colony optimization: A case study in Yili River Valley, China. Ecological Indicators, 169: 112770, doi: 10.1016/j.ecolind.2024.112770.

Pan J H, Liang J, Zhao C C. 2023. Identification and optimization of ecological security pattern in arid inland basin based on ordered weighted average and ant colony algorithm: A case study of Shule River Basin, NW China. Ecological Indicators, 154: 110588, doi: 10.1016/j.ecolind.2023.110588.

Qi X T, Khu S T, Yu P, et al. 2025. Integrating machine learning with the minimum cumulative resistance model to assess the impact of urban land use on road waterlogging risk. Journal of Hydrology, 654: 132842, doi: 10.1016/j.jhydrol.2025.132842.

Qian D W, Du Y G, Li Q, et al. 2021. Alpine grassland management based on ecosystem service relationships on the southern slopes of the Qilian Mountains, China. Journal of Environmental Management, 288: 112447, doi: 10.1016/j.jenvman.2021.112447.

Qu C, Xu J, Li W, et al. 2025. Integrating circuit theory and network modeling to identify ecosystem carbon sequestration service flow networks. Ecological Informatics, 87: 103077, doi: 10.1016/j.ecoinf.2025.103077.

Shen J K, Wang J Y, Wu T Y, et al. 2024. Building landscape ecological network with multi-scenario connectivity based on network fault tolerance index and networking technology in graph theory. Ecological Indicators, 166: 112417, doi: 10.1016/j.ecolind.2024.112417.

Shen Z, Wu W, Chen S F, et al. 2022. A static and dynamic coupling approach for maintaining ecological networks connectivity in rapid urbanization contexts. Journal of Cleaner Production, 369: 133375, doi: 10.1016/j.jclepro.2022.133375.

Song S, Xu D, Hu S S, et al. 2021. Ecological network optimization in urban central district based on complex network theory: A case study with the urban central district of Harbin. International Journal of Environmental Research and Public Health, 18(4): 1427, doi: 10.3390/ijerph18041427.

Sui X R, Xu Q L, Tao H, et al. 2024. Vegetation dynamics and recovery potential in arid and semi-arid Northwest China. Plants, 13(23): 3412, doi: 10.3390/plants13233412.

Sun D L, Wu X Q, Wen H J, et al. 2024a. Ecological security pattern based on XGBoost-MCR model: A case study of the Three Gorges Reservoir Region. Journal of Cleaner Production, 470: 143252, doi: 10.1016/j.jclepro.2024.143252.

Sun W J, Yu Q, Xu C L, et al. 2024b. Construction and optimization of ecological spatial network in typical mining cities of the Yellow River Basin: The case study of Shenmu City, Shaanxi. Ecological Process, 13: 60, doi: 10.1186/s13717-024-00539-z.

Tong A, Zhou Y, Chen T, et al. 2025. Constructing an ecological spatial network optimization framework from the pattern–process–function perspective: A case study in Wuhan. Remote Sensing, 17(15): 2548, doi: 10.3390/rs17152548.

Wang Y, Yu Q, Avirmed B, et al. 2025a. The response of ecosystem services to ecological spatial network patterns in China's arid and semi-arid regions. Ecological Indicators, 172: 113300, doi: 10.1016/j.ecolind.2025.113300.

Wang Y J, Qu Z Y, Zhong Q C, et al. 2022a. Delimitation of ecological corridors in a highly urbanizing region based on circuit theory and MSPA. Ecological Indicators, 142: 109258, doi: 10.1016/j.ecolind.2022.109258.

Wang Z C, Zhao X S, Cui L J, et al. 2025b. Identification and optimization of urban wetland ecological networks in highly urbanized areas: A case study of Haidian District, Beijing. Ecological Indicators, 170: 113028, doi: 10.1016/j.ecolind.2024.113028.

Wang Z X, Xiao L, Yan H M, et al. 2022b. Optimization of the ecological network structure based on scenario simulation and trade-offs/synergies among ecosystem services in Nanping. Remote Sensing, 14(20): 5245, doi: 10.3390/rs14205245.

Wanghe K Y, Guo X L, Wang M, et al. 2020. Gravity model toolbox: An automated and open-source ArcGIS tool to build and prioritize ecological corridors in urban landscapes. Global Ecology and Conservation, 22: e01012, doi: 10.1016/j.gecco.2020.e01012.

Wei Q, Halike A, Yao K X, et al. 2022. Construction and optimization of ecological security pattern in Ebinur Lake Basin based

on MSPA-MCR models. Ecological Indicators, 138: 108857, doi: 10.1016/j.ecolind.2022.108857.

Wei S R, Yu T, Ji P, et al. 2024. Analysis on ecological network pattern changes in the Pearl River Delta forest urban agglomeration from 2000 to 2020. Remote Sensing, 16(20): 3800, doi: 10.3390/rs16203800.

Wei W, Zhang Y L, Wei X X, et al. 2025. Construction and optimization of ecological security patterns based on ecosystem service function and ecosystem sensitivity in the important ecological functional area—A case study in the Yellow River Basin. Ecological Engineering, 215: 107609, doi: 10.1016/j.ecoleng.2025.107609.

Wei X T, Eboy O V, Cao G C, et al. 2023. Spatio-temporal variation of water conservation and its impact factors on the southern slope of Qilian Mountains. Regional Sustainability, 4(1): 54–67.

West S, Cairns R, Schultz L. 2016. What constitutes a successful biodiversity corridor? A Q-study in the cape floristic region, South Africa. Biological Conservation, 198: 183–192.

Wu Y H, Qin F C, Li L, et al. 2024. Construction and optimisation of watershed scale ecological network: A case study of Kuye River Basin. Frontiers in Environmental Science, 12: 1364568, doi: 10.3389/fenvs.2024.1364568.

Xiang Q, Yu H, Huang H, et al. 2024. Assessing the resilience of complex ecological spatial networks using a cascading failure model. Journal of Cleaner Production, 434: 140014, doi: 10.1016/j.jclepro.2023.140014.

Xu D M, Peng J, Dong J Q, et al. 2024. Expanding China's protected areas network to enhance resilience of climate connectivity. Science Bulletin, 69(14): 2273–2280.